Aggregating Synechococcus contributes to particle organic carbon export in coastal estuarine waters: Its lineage features and assembly processes

Ting Wang, Jialin Li, Yandong Xu, Tao Zou, Song Qin

PII: S0048-9697(24)00503-5

DOI: https://doi.org/10.1016/j.scitotenv.2024.170368

Reference: STOTEN 170368

To appear in: *Science of the Total Environment*

Received date: 5 December 2023

Revised date: 8 January 2024

Accepted date: 20 January 2024

Please cite this article as: T. Wang, J. Li, Y. Xu, et al., Aggregating Synechococcus contributes to particle organic carbon export in coastal estuarine waters: Its lineage features and assembly processes, *Science of the Total Environment* (2023), https://doi.org/10.1016/j.scitotenv.2024.170368

Aggregating *Synechococcus* Contributes to Particle Organic Carbon Export in Coastal Estuarine Waters: Its Lineage Features and Assembly Processes

Ting Wang[a,d], Jialin Li[a,*], Yandong Xu[b], Tao Zou[c], Song Qin[a,]**

[a] Key Lab of Coastal Biology and Biological Resource Conservation, Yantai Institute of Coastal Zone Research, Chinese Academy of Sciences, Yantai 264003, China

[b] Shandong Provincial Key Laboratory of Restoration for Marine Ecology, Shandong Marine Resource and Environment Research Institute, Yantai 264006, China

[c] Key Laboratory of Coastal Zone Environmental Processes and Ecological Remediation, Yantai Institute of Coastal Zone Research, Chinese Academy of Sciences, Yantai 264003, Shandong, China

[d] University of Chinese Academy of Sciences, Beijing 101408, China

***Correspondence:**

Jialin Li

jlli@yic.ac.cn

****Correspondence:**

Song Qin

sqin@yic.ac.cn

Abstract

The release and deposition of phytoplankton-derived particulate organic matter is crucial in marine carbon export, yet the roles of picoplankton in these processes were seldom considered. Therefore, this study aimed to shed light on the matter by investigating the aggregating (AG) lifestyle of *Synechococcus*, a main group of picoplankton, in the coastal waters of the Yellow River Estuary with ample sediments acting as ballast minerals. We revealed that AG *Synechococcus* constituted a substantial portion, maximally reaching up to 85.4%, of the total *Synechococcus* population. Pearson correlations and random forest (RF) regression analyses found significant connections ($p < 0.01$) between AG *Synechococcus* and the content of particulate organic carbon (POC), which emphasized its underlying role in facilitating POC export in this region. Furthermore, by employing high-throughput sequencing of the RNA polymerase gene (*rpo*C1), it was demonstrated that S5.1 clade I exhibited a significantly higher proportion in the AG fraction than in the free-living (FL) fraction ($p < 0.05$). This suggests distinct inclinations in the phylogenetic preference for different *Synechococcus* lineages between different lifestyles in the studied area. Finally, we ascertained "small-world" and higher robustness attributes of aggregates formed through the co-occurrence construction between *Synechococcus* and heterotrophic bacteria, likely facilitated by the reciprocal exchange of carbon and nitrogen elements. Overall, these findings have implications for our understanding of the role of *Synechococcus* in the ecology and biogeochemistry of marine ecosystems, and they are significant for more accurately evaluating the contribution of

picophytoplankton in ocean carbon export.

Keywords

Pico-cyanobacterial *Synechococcus*; Aggregating lifestyle; phylogenetic preference; particle organic matter

1. Introduction

Climate change stands as the foremost policy and scientific challenge at present (Dalpadado et al., 2024; Huang et al., 2018). Marine phytoplankton play a crucial role in climate regulation by taking up inorganic carbon through photosynthesis (Timmermann and Jin, 2002). The majority of the organic carbon (OC) generated by phytoplankton in the euphotic zone is consumed and remineralized *in situ*, while a portion is exported as sinking particulate organic matter (POM) (Cabrera-Brufau et al., 2021; Li et al., 2023b). The sinking process of POM is governed by phytoplankton features including cell size and shape, as well as the ballasting effect of minerals (Durante et al., 2019). Phytoplankton, such as Diatom, received significant attention, while picoplankton, characterized by smaller size and absence of natural ballast minerals, were often been neglected in POM sinking studies (Tréguer et al., 2018). Nonetheless, picoplankton, particularly *Synechococcus*, possess aggregation capacity that compensates for their individual small cell size (Cruz and Neuer, 2019; Deng et al., 2016). Simultaneously, clay and nonclay minerals in seawater can serve as their ballast minerals, thus facilitating the export of carbon (Deng et al., 2015). Moreover, the current studies recognize a projected future increase in the proportion and abundance of small-sized phytoplankton, including picoplankton (Morán et al., 2010). Consequently, it is imperative to intensify investigations into the processes and mechanisms of carbon export, particularly in small-sized phytoplankton, to improve our grasp of their role in carbon biogeochemical cycle and climate regulation within present and future marine ecosystems.

Synechococcus, a typical genus of Cyanobacteria, is abundant and extensively distributed throughout the global ocean (Scanlan et al., 2009). As a photosynthetic prokaryote, *Synechococcus* plays a crucial role in global carbon fixation, contributing 16.7% to the ocean's net primary production (Flombaum et al., 2013). In particular, its contributed production of total primary production in the coastal region can be even higher (Tsai et al., 2012). A portion of organic carbon fixed by *Synechococcus* is transformed into "blue carbon" through the biological pump (BP) and microbial carbon pump (MCP) pathways, enabling long-term storage in marine environments (Deng et al., 2015; Zhao et al., 2017). Despite its diminutive size, absence of inherent ballasting mineral particles, and lack of close association with micrograzers, *Synechococcus* was initially considered insignificant in marine particulate organic carbon (POC) contribution through the BP pathway (Worden and Binder, 2003). Nevertheless, research increasingly emphasizes its role in POC flux due to aggregate formation (Amacher et al., 2013; Deng et al., 2015; Li et al., 2023a). With sufficient ballasting minerals such as calcium carbonate, opal, and lithogenic material, part *Synechococcus* can form aggregates as large as 1.4 millimeters in diameter, sinking at speeds of up to 440 m d^{-1} (Deng et al., 2015). This rate is comparable to sinking rates observed for diatoms (Hamm, 2002) and coccolithophores (Iversen and Ploug, 2010) in similar experiments and marine snow *in situ* (Alldredge and Gotschalk, 1988). These studies underscore the importance of aggregating lifestyle *Synechococcus* in carbon export in laboratory experiments. However, the actual contribution of these *Synechococcus* in the BP pathway at ecological scales, particularly in ballast mineral-

rich regions like estuaries, requires further investigation.

Marine *Synechococcus* displays high phylogenetic diversity, and it can be classified into three main subclusters: S5.1, S5.2, and S5.3 (Dufresne et al., 2008). Each subcluster consists of various clades, with S5.1 harboring the highest number of identifiable clades (Wang et al., 2022c). Different *Synechococcus* lineages demonstrate varying metabolic capabilities, encompassing carbon fixation, organic nutrient utilization, chromatic acclimation, and so on (Chen et al., 2022; Mackey et al., 2017). As a result, these lineages exhibit diverse niche preferences and adaptive features in global oceans (Six et al., 2021; Wang et al., 2022d; Xia et al., 2017). Nevertheless, it remains unclear the aggregation preferences of distinct *Synechococcus* lineages. Besides, *Synechococcus* and heterotrophic bacteria establish close and intricate interactions that involve in nutrient exchange and signal transduction (Nair et al., 2022; Te et al., 2023; Xia et al., 2021). In particular, certain interactions have been observed to induce *Synechococcus* flocculation and aggregation, playing a crucial role in regulating the carbon export of *Synechococcus* in the marine environment, but the precise processes and mechanisms require further exploration (Cruz and Neuer, 2019; Zhang et al., 2021).

The Yellow River was the second-largest global river in terms of sediment flux, supplying 6% of the oceans' sediment input over millennia (Liu et al., 2012). Despite an over 80% reduction in the sediment transport of the Yellow River caused by human activities (reservoir constructions, water-soil conservation, etc.) in recent years, substantial sediment continues to be deposited from the Yellow River into the Bohai

Sea annually (Wang et al., 2022a). The sediment transported by the Yellow River contains clay and nonclay minerals such as silicon and calcium compounds that can act as ballast minerals (Tian et al., 2021). This makes the coastal area of the Yellow River Estuary an ideal region for studying the aggregation and sinking of *Synechococcus*. In this study, by size-fractionating seawater samples, we investigated the contrasting lifestyles of *Synechococcus* within the coastal waters of the Yellow River Estuary. According to the aggregation experiment of Deng et al., (2016), *Synechococcus* aggregates, as observed under epifluorescence microscopy, exhibited a size range from 3 μm to over 100 μm. Consequently, we categorized those capable of passing through a 3 μm filter membrane as inclined towards a free-living (FL) lifestyle, while those retained tended to adopt an aggregating (AG) lifestyle in this study. Our primary objectives were: 1) to investigate the distribution discrepancies between AG and free-living FL *Synechococcus* and their respective contributions to POC; 2) to uncover the dominant phylogenetic lineages and community turnover progress of the two *Synechococcus* lifestyles; and 3) to explore the underlying aggregate mechanism of AG *Synechococcus* in terms of interactions with co-occurring heterotrophic bacteria.

2. Materials and methods

2.1 Sampling and laboratory analyses

2.1.1 Sample collections

Field sampling was conducted aboard the research vessel Chuangxin Yi in the coastal waters of the Yellow River estuary from November 5 to 11, 2022 (**Figure S1**). Seawater samples were collected from the surface and bottom layers at each station using a conductivity, temperature, and depth (CTD) rosette sampler (Sea-Bird 911Plus, Sea-Bird Electronics Inc., Bellevue, WA, USA) equipped with Niskin bottles. The samples were prefiltered through a 48-μm nylon mesh to remove microphytoplankton prior to downstream treatment. Accurate 1.0 mL of filtered (through 3-μm syringe filters) or nonfiltered seawater was pipetted and fixed with paraformaldehyde (final concentration, 0.5%) for the measurement of FL (< 3 μm) or total microbial abundance, respectively. About 1 L of seawater was initially filtered through 3-μm (AG) and 0.22-μm (FL) pore-size polycarbonate membranes (Millipore Co., Bedford, MA, USA) to collect the two size fractions. The membranes were rapidly frozen in liquid nitrogen and subsequently stored at −80°C until DNA extraction. For particulate matter analysis, accurate 1 L of seawater was collected on precombusted (450°C for 10 h) 0.7-μm pore-size GF/F filters (47 mm diameter; Whatman). The filters were placed in petri dishes and stored at −20°C until further analysis. The filtered water was collected in precombusted (450°C for 10 h) 40 mL glass vials and stored at −20°C for total dissolved carbon (TDC) and dissolved organic carbon (DOC) analysis. For total chlorophyll *a* (chl *a*) analysis, 1 L of seawater was filtered through 0.7-μm pore-size GF/F filters (47 mm diameter; Whatman). The filters were stored at −20°C until further analysis. Approximately 50 mL of seawater filtered through 0.22-μm pore-size polycarbonate membranes was collected and stored at −20°C for

nutrient measurement.

2.1.2 Environment parameter measurement

The physicochemical parameters, including temperature, salinity, depth, pH, turbidity, and oxygen saturation, were recorded *in situ* with a CTD (Sea-Bird, USA). The chl *a* concentration was determined using a Trilogy Laboratory Fluorometer (Turner Designs, USA) after extraction in 90% acetone at 4°C in the dark for 20 h (Chen et al., 2009). Inorganic nutrients, including NO_2^-, NO_3^-, NH_4^+, PO_4^{3-}, and SiO_3^{2-}, were measured using a continuous flow analyzer (Seal-Branlubbe AA3, Seal, Germany) (Dafner, 2015). Concentrations of TDC and DOC in the filtrate were measured using a total organic carbon analyzer (Vario TOC select, Elementar, Germany) (Cai et al., 2015). For DOC measurements, the samples were acidified with concentrated HCl to a pH <2 before analysis. Samples were not acidified for TDC measurements. Concentrations of dissolved inorganic carbon (DIC) were calculated as the difference between TDC and DOC concentrations. After freeze-drying and acid-fuming, the GF/F filters were measured for the concentrations of particulate organic carbon (POC) using an elemental analyzer (Vario MACRO cube, Elementar). CTD, nutrient, and chl *a* data were graciously provided through the cruise-sharing collaboration.

2.1.3 Abundance measurement of *Synechococcus* and heterotrophic bacteria

Abundance samples were measured using a BD FACSAria™ flow cytometer (FCM). The aggregates in each sample were dispersed and homogenized via shaking and oscillating before FCM analysis. The abundance of *Synechococcus* was determined by

detecting their autofluorescence emitted at 580 ± 30 nm (FL2, orange fluorescence, phycoerythrin) and > 650 nm (FL3, red fluorescence, chlorophyll *a*) (Ruber et al., 2018). The abundance of heterotrophic bacteria was determined by detecting green fluorescence emitted at 530 ± 30 nm (FL1) after staining with SYBR Green I DNA dye (Marie et al., 1997). Yellow–green fluorescent beads (2.0 μm, Polysciences, Warrington, PA, USA) were added as the instrument's internal standard. Data and plots were processed and exported using the cytometer analysis program WinMDI software 2.9 (Joseph Trotter, Scripps Research Institute, La Jolla, CA, United States). The abundances of AG *Synechococcus* or heterotrophic bacteria were calculated as their difference between total and FL abundance, respectively.

2.1.4 Molecular experiment

DNA extraction was performed using an E.Z.N.A.® Soil DNA Kit (Omega Biotek, USA) (Zhang et al., 2015). Polymerase chain reaction (PCR) was carried out in an ABI GeneAmp® 9700 PCR thermocycler (ABI, CA, USA). Amplification of *Synechococcus rpo*C1 gene sequences was performed with the *rpo*C1-39F (5′-GGNATYGTYTGYGAGCGYTG-3′) and rpoC1-462R (5′-CGYAGRCGCTTGRTCAGCTT-3′) primer pair, as previously described (Wang et al., 2022b). Amplification of the V3-V4 region of 16S rRNA gene sequences was performed with the 341F (5′-CCTAYGGGRBGCASCAG-3′) and 806R (5′-GGACTACNNGGGTATCTAAT-3′) primer pair, as previously described elsewhere (Sundberg et al., 2013). The resulting amplicons were gel purified, quantified, pooled, and finally paired-end sequenced (2×250 bp) on an Illumina NovaSeq PE250 platform

(Shanghai Biozeron Co., Ltd., China), following standard protocols.

2.2 Statistical analysis and visualizations

2.2.1 Sequence analysis

Raw demultiplexed forward and reverse reads were processed with the microbiome bioinformatics platform QIIME2 (https://library.qiime2.org) (Bolyen et al., 2019). The open-source software package Dada2 (https://github.com/benjjneb/dada2) was used for sequence quality control and amplicon sequence variant (ASV) clustering (Callahan et al., 2016). Taxonomic assignment of 16S phylotypes was performed using a Bayesian Classifier trained (Bokulich et al., 2018) with Silva database version 138 (99% OTUs full-length sequences) (https://www.arb-silva.de/) (Robeson et al., 2021). ASVs belonging to Chloroplast and Cyanobacteria were deleted for better statistics of the heterotropic bacterial community. For the taxonomic assignment of *rpo*C1 gene sequences, the representative sequence of each ASV was blasted against a self-built database (Wang et al., 2022b). The unclassified sequences were deleted. Phylogenetic information of referenced strains was obtained from the Roscoff Culture Collection (http://roscoff-culture-collection.org/strains/shortlists/taxonomic-groups/marine-*Synechococcus*). Alpha diversities were calculated based on the feature tables produced by package *vegan* in R Language 4.2.2 (Oksanen et al., 2022). A graphical software package (statistical analysis of taxonomic and functional profiles, STAMP) was used for the Wilcoxon rank sum test to test significantly different taxonomic profiles between AG and FL groups (Parks et al., 2014).

2.2.2 Microbial turnover evaluation

Populations' phylogenetic turnover was evaluated following the previous description (Stegen et al., 2013) using the R package *picante* (Kembel et al., 2010). First, the observed beta-mean-nearest taxon distance (βMNTD) was calculated through the utilization of the ASV table and phylogenetic trees. Subsequently, we computed the values of randomized (Null) βMNTD using a null distribution model across the phylogeny 999 times. Finally, we determined the beta nearest taxon index (βNTI) by calculating the standard deviations between the observed βMNTD and the mean of the null βMNTD. A |βNTI| value > 2 indicates that phylogenetic turnover exceeds expectations and is influenced by deterministic processes. Conversely, a |βNTI| value < 2 indicates that phylogenetic turnover aligns with stochastic expectations, implying that turnover is primarily influenced by stochastic processes. When |βNTI|< 2, it is necessary to perform additional calculations of the Raup–Crick index based on Bray-Curtis dissimilarity (RCbray). This computation aids in discerning the stochastic components of assembly into homogenizing dispersal, dispersal limitation, and undominated processes. Undominated processes are characterized by indexes |βNTI| < 2 and |RCbray| < 0.95, encompassing a combination of stochastic processes including weak selection/dispersal, diversification, and drift (Huang et al., 2022).

2.2.3 Environmental explanation of microbial variation

The R packages *psych* (Revelle, 2023) and *pheatmap* (Kolde, 2019) were used to generate correlation heatmaps between microbial abundance and environmental

factors. To reveal the constraints of different microbial abundances on POC variation, RF analysis was conducted with 1000 decision trees using the R package *randomForest* (Liaw and Wiener, 2002). The increase in mean squared error (%IncMSEs) for each variable indicated its importance to POC variation. Variance inflation factor (VIF) analysis was conducted to eliminate the effect of collinearity among environmental parameters using the R package *car* (Fox and Weisberg, 2019). Redundancy analysis (RDA) was used to explore the variation explanation of microbial communities by environmental factors using the R package *vegan* (Oksanen et al., 2022). Microbial community data were Hellinger transformed to improve homoscedasticity and normality for the RDA.

2.2.4 Co-occurrence network construction

To estimate the interactions of *Synechococcus* lineages and heterotrophic microbial communities between the AG and FL groups, corresponding combination co-occurrence networks were constructed encompassing the top 200 abundant heterotrophic microbial genera and all *Synechococcus* lineages. Correlation matrices were constructed by calculating all possible pairwise Spearman's rank correlations among AG or FL communities after standardization using the package *dplyr* (Wickham et al., 2023). When Spearman's correlation coefficient (ρ) was > 0.6 and the p value was < 0.05, statistical robustness was considered to exist between the two items. Network analysis was conducted using the packages *ggClusterNet* (Wen et al., 2022) and *igraph* (Csardi et al., 2023), and the Gephi interactive platform was used to perform the network visualization. The dynamics of microbial network robustness

were computed by calculating the proportion of remaining nodes and natural connectivity after randomly removing a certain proportion or number of nodes, which were calculated and visualized using the packages *pulsar* (Müller et al., 2016) and *patchwork* (Pedersen, 2023).

2.2.5 Function prediction

Functional annotation of taxa was performed using the program "functional annotation of prokaryotic taxa" (FAPROTAX) on ASV table (Louca et al., 2016). FAPROTAX is a manually constructed database that maps prokaryotic taxa (e.g., genera or species) to putative functions based on the literature on cultured representatives. It was believed that predicting putative functional groups using this approach is superior to genomic prediction approaches based on sequence homology (Kumar et al., 2019). Linear fitting analysis between the relative abundance of *Synechococcus* lineages and ecological function was conducted using the R package *ggtrendline* (Mei et al., 2022).

3. Results

3.1 Environmental conditions of the sampling stations

The environmental conditions showed large variation among sampling stations, while differences between water layers within each station were relatively minor (**Figure S2**). Stations Y1, Y3, D4, and L11 are situated at a distance from the estuary, making them more influenced by seawater. These stations exhibited higher salinity (28.9 ± 0.5)

and temperature (15.2 ± 0.3 ℃), but lower carbon content, including DIC (14.5 ± 0.6 mg L^{-1}), DOC (4.6 ± 0.4 mg L^{-1}), and POC (5.5 ± 0.9 mg L^{-1}), as well as lower nutrient concentrations, including NO_2^- (2.1 ± 0.6 ×10^{-2} mg L^{-1}), NO_3^- (9.4 ± 6.5 ×10^{-2} mg L^{-1}), NH_4^+ (2.8 ± 0.8 ×10^{-2} mg L^{-1}), and SiO_3^{2-} (7.4 ± 2.9 ×10^{-2} mg L^{-1}). Stations B1, C1, D1, and E2 are located near the estuary and are influenced considerably by the input of fresh water and sediment from the Yellow River. These stations had lower salinity (25.7 ± 0.6), but higher turbidity (19.7 ± 19.3), POC (10.7 ± 7.7 mg L^{-1}), and nutrient concentrations, particularly NO_2^- (2.8 ± 0.7 ×10^{-2} mg L^{-1}) and NH_4^+ (4.9 ± 0.9 ×10^{-2} mg L^{-1}). Specifically, the C1 station, being the closest to the Yellow River Estuary, exhibited the highest turbidity (47.0 ± 24.3) and POC (22.1 ± 7.3 mg L^{-1}). Station L03 is situated in Laizhou Bay, where it accumulates fresh water and sediment from the Yellow River. It exhibited the lowest salinity (21.6 ± 0.0) and temperature (13.2 ± 0.1℃), but the highest concentrations of DOC (6.3 ± 0.3 mg L^{-1}), DIC (16.2 ± 0.4 mg L^{-1}), SiO_3^{2-} (33.5 ± 3.0 ×10^{-2} mg L^{-1}), and NO_3^- (84.3 ± 10.0 ×10^{-2} mg L^{-1}).

3.2 The abundance of *Synechococcus* and heterotrophic bacteria

The abundance of total *Synechococcus* in the study area ranged from 1.1 to 4.1 ×10^4 cells mL^{-1} (**Figures 1A** and **B**). The highest total abundance was found at the C1 station located closest to the estuary, while the lowest was at the Y3 station, situated farther from the estuary. The AG *Synechococcus* accounted for 14.7% to 85.4% of the total *Synechococcus*. Overall, the mean abundance of AG *Synechococcus* (1.2 ± 0.9 ×10^4 cells mL^{-1}) was higher than that of FL *Synechococcus* (0.8 ± 0.3 ×10^4 cells mL^{-1}),

while no significant difference was found between AG and FL fractions in the studied area. Nevertheless, we found that the abundance of AG *Synechococcus* (1.7 ± 1.1 $\times 10^4$ cells mL^{-1}) was significantly higher than that of FL *Synechococcus* (0.6 ± 0.1 $\times 10^4$ cells mL^{-1}) at stations near the estuary (B1, C1, D1, and E2) (T test, $p < 0.05$). The differences in *Synechococcus* abundance between water layers within each station were not obvious. However, at station L03 in Laizhou Bay, the abundance of AG *Synechococcus* was lower in the surface water layer but higher in the bottom water layer compared to FL *Synechococcus*.

The abundance of total heterotrophic bacteria ranged from 1.7 to 6.4 $\times 10^5$ cells mL^{-1} (**Figures 1C** and **D**). The AG heterotrophic bacteria accounted for 12.1% to 65.3% of the total heterotrophic bacteria. AG heterotrophic bacteria (1.4 ± 0.7 $\times 10^5$ cells mL^{-1}) exhibited significantly lower abundance than FL *Synechococcus* (2.5 ± 1.2 $\times 10^4$ cells mL^{-1}, T test, $p < 0.05$).

3.3 The community characteristics of *Synechococcus* and heterotrophic taxa

Amplicon sequencing of the *rpo*C1 gene generated 715,796 clean sequences from 20 samples, with Good's coverage over 99.9% for each sample, indicating nearly complete coverage (**Table S1**). The various alpha-diversity indexes were higher in the AG *Synechococcus* community than in the FL *Synechococcus* community (**Table S1 and Figure S3**). A total of 14 lineages were identified, including ten clades of S5.1, as well as S5.2, S5.3, *Cyanobium*, and freshwater *Synechococcus* (FS) (**Figures 2A** and **B**). All three subclusters of marine *Synechococcus* were detected at each station, with

Synechococcus S5.1 being the predominant subcluster across all stations. Among the 10 identified clades of *Synechococcus* S5.1, clade III was the most abundant, followed by clades I, IX, and HK1. Clades V, VI, VII, and VIII were rare lineages, with mean proportions of less than 1%. Compared to the FL *Synechococcus* community, AG *Synechococcus* had higher relative abundances of S5.1 clades I and VI, S5.2, S5.3, and FS. In contrast, the other nine lineages had more relatives in the FL *Synechococcus* community. In particular, based on the Wilcoxon rank sum test, we found a significantly different proportion of S5.1 clade I between AG and FL samples ($p < 0.05$) (**Figures 2C**).

Amplicon sequencing of the V3–V4 hypervariable region of the bacterial 16S rRNA gene generated 744,972 clean sequences from 20 samples, with Good's coverage over 99.9% for each sample (**Table S2**). The various alpha-diversity indexes were not obviously different between the AG and FL bacterial communities (**Table S2 and Figure S4**). Taxonomic assignment showed that Proteobacteria was the most abundant phylum among all samples, reaching a mean proportion of 67.1% (**Figure S5**). Among this phylum, Alphaproteobacteria was the most abundant class, followed by Gammaproteobacteria.

3.4 The effect of environmental variables

The abundance of FL *Synechococcus* showed a significant correlation with DIC ($\rho = 0.57$, $p < 0.05$), whereas AG *Synechococcus* abundance was significantly correlated with POC ($\rho = 0.88$, $p < 0.01$), turbidity ($\rho = 0.80$, $p < 0.01$), and NO_2^- concentration

(ρ = 0.57, p < 0.05) (**Figure 3A**). The RF analysis, using 1000 decision trees, revealed that the four abundances collectively constrained 40.9% of the variation in POC (**Figure 3B**). The increase in mean squared error (%IncMSEs) for each variable indicated its importance to POC variation, with AG *Synechococcus* abundance showing the highest %IncMSEs value.

After conducting VIF analysis, environmental variables with strong self correlations were excluded, and seven other environmental variables, depth, chl *a*, PO_4^{3-}, NH_4^+, DIC, DOC, and POC, without multicollinearity were retained for conducting RDA (VIF values < 10). The first two axes of RDA accounted for 61.15% of the total variance of AG *Synechococcus* assemblage (**Figure 3C**), which is less than that of FL *Synechococcus* assemblage (63.08%, **Figure 3D**). The AG *Synechococcus* assemblage had a significant correlation with POC (ρ = 0.86, p < 0.01), while none of the seven environmental variables showed a significant correlation with the FL *Synechococcus* assemblage.

3.5 Turnover processes of *Synechococcus* and bacterial community

Both βMNTI and βNTI were significantly higher in FL *Synechococcus* than in AG *Synechococcus* communities (T test, p < 0.05) (**Figures 4A** and **B**). *Synechococcus* populations in the coastal waters of the Yellow River estuary were more governed by stochastic processes for the AG fraction. The mean Raup-Crick probability index was also higher in FL *Synechococcus* populations than in AG *Synechococcus* populations (**Figure 4C**). AG *Synechococcus* turnover was affected by 4% homogenizing

dispersal (RCbray < −0.95), 29% dispersal limitation (RCbray > 0.95), and 67% undominated processes in the whole area (|RCbray| < 0.95). FL *Synechococcus* turnover was affected by 11% homogenizing dispersal, 36% dispersal limitation, and 40% undominated processes.

The βMNTI, βNTI, and Raup-Crick probability index were not significantly different between the AG and FL bacterial communities (**Figure S6**). The AG and FL fractions displayed 11% and 16% deterministic processes, respectively. In contrast to the *Synechococcus* community, both AG and FL bacterial communities' turnover was mostly affected by the dispersal limitation of stochastic processes.

3.6 Microbial co-occurrence

To estimate the coexistence of *Synechococcus* lineages and heterotrophic genera at different fractions, co-occurrence networks were established for both AG (**Figure 5A**) and FL (**Figure 5B**) communities. Both AG and FL networks consisted of 213 nodes. The AG network was linked by 4,221 edges, while the FL network displayed fewer edges (3,255). Tropological parameters, including average degree, connectance, mean clustering coefficient, and relative modularity, exhibited significantly higher values in AG samples than in FL samples (T test, $p < 0.01$) (**Figure S7**). However, the value of the average path length was significantly lower in AG samples than in FL samples (T test, $p < 0.01$). The AG network exhibits a high mean clustering coefficient and low average path length, indicating pronounced 'small-world' features characterized by abundant connection clustering and short distances between nodes. This illustrates the

AG network's capability to facilitate the swift distribution of perturbation effects across the entire network, optimizing overall system efficiency (Yuan et al., 2021).

Taxa extinction was simulated by randomly removing nodes and then the network stability was examined by calculating the remaining nodes (**Figure 5C**) and the natural connectivity indexes (**Figure 5D**) after node removal. The results showed that the AG network exhibited greater robustness, regardless of the proportion of nodes removed.

3.7 Bacterial function prediction and relationship with *Synechococcus* lineages

The FAPROTAX database was utilized for annotation and functional screening of bacterial communities involved in carbon, nitrogen, hydrogen, and sulfur cycles in the AG (**Figure 6A**) and FL (**Figure 6B**) fractions. The carbon cycle functions primarily encompassed chemoheterotrophy, aerobic chemoheterotrophy, methanol oxidation, and methylotrophy. Nitrogen cycle functions consisted mainly of nitrate respiration, nitrogen respiration, and nitrate reduction. Hydrogen cycle functions were limited to dark hydrogen oxidation, and sulfur cycle functions predominantly included dark sulfide oxidation and dark oxidation of sulfur compounds. Through linear regression analysis between *Synehcococcus* clade I and various ecological functions, we identified significant linear relationships between this lineage and chemoheterotrophy ($R^2 = 0.23$, $p < 0.05$), nitrogen fixation ($R^2 = 0.28$, $p < 0.05$), and ureolysis ($R^2 = 0.23$, $p < 0.05$) (**Figure 6C**).

4. Discussion

4.1 The underlying contribution of AG *Synechococcus* in POC export in coastal waters of the Yellow River estuary

Our results demonstrate that a noteworthy proportion of *Synechococcus* (ranging from 14.7% to 85.4%) preferentially form aggregates larger than 3 μm in coastal waters of the Yellow River estuary (**Figures 1 and 7**). There was a clear spatial gradient in the distribution of the AG cells with the more abundant in near the estuary. The abundance of AG *Synechococcus* significantly surpasses that of FL *Synechococcus* at stations near the estuary with high turbidity (T test, $p < 0.05$). The abundance of AG *Synechococcus* was linked to changing turbidity ($\rho = 0.80$, $p < 0.01$). Similar patterns have been observed in other estuarine environments (Liu et al., 2014; Mao et al., 2022). This phenomenon could be attributed to the enhancement of suspended minerals contributing to the flocculation of *Synechococcus* aggregates *in situ* (Deng et al., 2015). Previous aggregation experiments also revealed the aggregation phenomenon in the presence of the ballasting mineral kaolinite and high *Synechococcus* abundance (Cruz and Neuer, 2019). Besides, a positive correlation between AG *Synechococcus* and NO_2^- concentration ($\rho = 0.57$, $p < 0.05$) implied that river input could provide inorganic nutrients, fostering the rapid growth of AG *Synechococcus* (Xie et al., 2020). In comparison, the abundance of FL *Synechococcus* was associated with DIC ($\rho = 0.57$, $p < 0.05$). This could be a result of the higher expression of carboxysomes of FL *Synechococcus* under higher levels of DIC, reflecting its more active carbon fixation in low-turbidity water conditions (Mao et al.,

2022).

The BP process involves the photosynthetic fixation of CO_2 to POC by phytoplankton and the export of POC to the ocean's interior (Li et al., 2023b; Wei et al., 2022). *Synechococcus* is a significant carbon fixation contributor in oceans, while it has not traditionally been regarded as a substantial contributor to oceanic carbon export due to their small size (Worden and Binder, 2003). Nonetheless, our results found that both Spearman's correlations between microbial abundance and environmental variables, as well as the variable importance in POC using RF regression, unveil a significant correlation between AG *Synechococcus* and POC content (**Figure 3**), which suggested the underlying contribution of AG *Synechococcus* to POC export in this region with a mass of sediments and sands as ballast minerals. Previous studies have also proposed that *Synechococcus* contributes to oceanic carbon export in proportion to their net primary production, achieved through the formation and gravitational sinking of aggregates (DuRand et al., 2001). Aggregates derived from *Synechococcus* were estimated to account for 2–13% of the total POC flux recorded by sediment traps at the Bermuda Atlantic Time-series Study site (Brew et al., 2009). DNA-based molecular analyses of sediment trap material also confirmed the role of *Synechococcus* in sinking particle flux (Amacher et al., 2013; De Martini et al., 2018). Based on carbon content per cell and the net growth rate of *Synechococcus* measured in adjacent waters (Tsai et al., 2012), our findings estimate that the underlying proportion of POC exports contributed by AG *Synechococcus* to total organic carbon burial could maximally reach 2.1% to 23% in the studied area (Hu et al., 2016).

However, we acknowledge the calculation is very rough due to potential variations in *Synechococcus* cellular carbon content and growth rate across different marine regions. Additionally, the impact of predation on their grazer has not been considered. Nonetheless, we can underscore the pivotal role of *Synechococcus* as a contributor to carbon sink in coastal carbon cycling. *Synechococcus* abundance is predicted to further increase in the marine ecosystem as the future climate changes caused by anthropogenic, environmental, and biological interactions (Flombaum and Martiny, 2021). Consequently, its contribution could be more substantial in the future. It is imperative to further investigate the processes of growth and being preyed on of *Synechococcus* in the studied area to provide a more precise estimation of its BP carbon sink potential. Additionally, exploring whether the same phenomenon exists on larger seasonal and spatial scales should also be taken into consideration.

4.2 The disparity in lineage compositions between AG and FL *Synechococcus* assemblages

Synechococcus displays high phylogenetic diversity, with various lineages exhibiting diverse geographic distributions and metabolic capabilities (Dufresne et al., 2008; Wang et al., 2022c). In this study, by employing high-throughput sequencing to analyze the *rpo*C1 gene, we unveiled distinct preferences in the proportion of different *Synechococcus* lineages between AG and FL samples (**Figures 2 and 7**). Specifically, in AG samples, we observed a higher prevalence of *Synechococcus* S5.1 clades I and VI, S5.2, S5.3, and FS compared to S5.1 clades III, IX, and HK1. Notably, the proportion of S5.1 clade I was significantly greater in AG samples than in FL

samples ($p < 0.05$). Previous research identified *Synechococcus* S5.1 clade I as a dominant lineage on a global scale, primarily restricted to higher latitudes and coastal regions at approximately 30 °N or 30 °S (Wang et al., 2022b; Wang et al., 2022c). This lineage is characterized by cold adaptation (Six et al., 2021), possibly accounting for its aggregation preference, as previous studies have identified the aggregating of bacterial cells to flocs in low-temperature environments (Alawi et al., 2007). However, the accurate physiological properties and molecular mechanisms that drive their tendency to aggregate in the studied area require further investigation through controlled experiments and omics analysis. Furthermore, our findings indicate that the assembly and turnover of the AG *Synechococcus* community were predominantly influenced by dispersal limitation (29%) and undominated processes (67%, induced by weak selection/dispersal, diversification, and drift) of stochastic processes rather than deterministic processes (**Figure 4**). These results suggest that different *Synechococcus* lineages could exhibit varying preferences for aggregation, and the formation of aggregates likely arises from the opportunistic coupling of lineages with aggregating potential in the studied area. However, a comprehensive understanding of the mechanism requires additional controlled experiments.

4.3 The potential assembly and sinking processes of the aggregations

The aggregation process could develop within a matrix of sticky organic substances referred to as transparent exopolymer particles (TEPs), a category of exopolymers abundant in acidic polysaccharides (Cruz and Neuer, 2019; Zamanillo et al., 2019). Although *Synechococcus* is the primary source of TEP, bacteria also have the capacity

to release TEP and its exopolymeric substance (EPS) precursors (Ortega-Retuerta et al., 2019). Interactions between them are believed to significantly influence the formation and characteristics of sinking aggregates, thus governing the fate of fixed carbon in aquatic ecosystems (Cruz and Neuer, 2019; Simon et al., 2002). Our findings align with this perspective. By constructing co-occurrent networks between *Synechococcus* and heterotrophic bacteria, we determined that aggregates formed with the co-occurrence of *Synechococcus* and heterotrophic bacteria are marked by a more abundant clustering of connections and shorter average distances between nodes, reflecting a "small-world" characteristic (**Figures 5 and 7**). Additionally, simulated taxon extinction through random node removal showed that the interactions between *Synechococcus* and heterotrophic bacteria contribute to more stable and robust aggregates. These interactions are likely underpinned by their exchange of C-N elements, as supported by the results of function prediction and data fitting which indicated significant linear relationships between the AG-preferred lineage and chemoheterotrophy, nitrogen fixation, and ureolysis bacteria (**Figure 6**). Recent studies have also illuminated that heterotrophic bacteria can sustain prolonged *Synechococcus* growth by establishing metabolic mutualism for nutrient exchange (Nair et al., 2022).

The previously posited "ballast hypothesis" proposes that the subsequent sinking of aggregates is quantitatively linked to suspended minerals, which are thought to heighten aggregate density, shield it from microbial degradation, and consequently impact its vertical movement through the water column (Armstrong et al., 2001).

Intriguingly, minerals found in sediment carried by rivers can serve as ballast minerals, making coastal waters of global estuaries a crucial area for the sinking of *Synechococcus* aggregates, which requires more attention. However, sediment transport is gradually diminishing due to anthropogenic activities such as dam and reservoir construction (Wang et al., 2016). Dam regulations have resulted in a ~5 Gt/yr reduction in sediment flux to the coastal ocean by the 21st century (Syvitski and Kettner, 2011). Consequently, our study implied that while a reduction in sediment load may improve light conditions and primary production in aquatic ecosystems, an overly dam-centric regulation of water-sediment may not only contribute to significant delta erosion but also result in a decline in the global-scale BP carbon sink. This decline is attributed to the lack of essential ballast minerals necessary for the flocculation and sinking of pico-plankton (Wang et al., 2017). Identifying the critical sediment load point is crucial for preserving the equilibrium between photosynthesis and carbon sinking in the coastal estuarine ecosystem. Meanwhile, a potential strategy for enhancing oceanic BP involving the use of clay minerals, termed the mineral-enhanced biological pump (MeBP), has been proposed (Yuan and Liu, 2021). Our research potentially lays a theoretical basis for this strategic approach.

5. Conclusion

In this study, we delved into the distribution, community characteristics, and interactions with heterotrophic bacteria of divergent lifestyles of *Synechococcus*

through size-fractionating seawater samples within the coastal waters of the Yellow River Estuary. The results showed that terrigenous sediment transport has an important effect on POC export of AG *Synechococcus* in coastal estuarine waters of the Yellow River. Distinct *Synechococcus* lineages exhibited different preferences between AG and FL lifestyles. C-N metabolism coupling between AG *Synechococcus* and bacteria could promote the assembling of aggregations. These findings are significant for more accurately evaluating the contribution of picophytoplankton in coastal carbon export. Furthermore, the results underscore the importance of factoring in sediment transport balance in river reservoir construction and offer theoretical support for the MeBP hypothesis.

Data availability

The sequence data for this study were deposited in the sequence read archive of NCBI, with a bio-project associated with this study having been applied for and processed in NCBI with the accession number PRJNA1034794. All raw sequencing data were stored under this bio-project.

Acknowledgments

This study is financially supported by the National Natural Science Foundation of China (No. 42176131) and the seed project of Yantai Institute of Coastal Zone Research, Chinese Academy of Sciences (No. YICE3510303). Data and samples were collected onboard of R/V Chuangxin I implementing the open research cruise NORC 2022-304 supported by NSFC Shiptime Sharing Project (project number: 42149301). The data analysis is supported by High-Performance Computing Platform of Yantai Institute of Coastal Zone Research, Chinese Academy of Sciences.

Declaration of interests

The authors declare that they have no known competing financial interests or personal relationships that could have appeared to influence the work reported in this paper.

References

Alawi M, Lipski A, Sanders T, Eva Maria P, Spieck E. Cultivation of a novel cold-adapted nitrite oxidizing betaproteobacterium from the Siberian Arctic. The ISME Journal 2007; 1: 256-264.

Alldredge AL, Gotschalk C. *In situ* settling behavior of marine snow. Limnology and Oceanography 1988; 33: 339-351.

Amacher J, Neuer S, Lomas M. DNA-based molecular fingerprinting of eukaryotic protists and Cyanobacteria contributing to sinking particle flux at the Bermuda Atlantic time-series study. Deep Sea Research Part II: Topical Studies in Oceanography 2013; 93: 71-83.

Armstrong RA, Lee C, Hedges JI, Honjo S, Wakeham SG. A new, mechanistic model for organic carbon fluxes in the ocean based on the quantitative association of POC with ballast minerals. Deep Sea Research Part II: Topical Studies in Oceanography 2001; 49: 219-236.

Bokulich NA, Kaehler BD, Rideout JR, Dillon M, Bolyen E, Knight R, et al. Optimizing taxonomic classification of marker-gene amplicon sequences with QIIME 2's q2-feature-classifier plugin. Microbiome 2018; 6: 1-17.

Bolyen E, Rideout JR, Dillon MR, Bokulich NA, Abnet CC, Al-Ghalith GA, et al. Reproducible, interactive, scalable and extensible microbiome data science using QIIME 2. Nature Biotechnology 2019; 37: 852-857.

Brew H, Moran S, Lomas M, Burd A. Plankton community composition, organic carbon and thorium-234 particle size distributions, and particle export in the

Sargasso Sea. Journal of Marine Research 2009; 67: 845-868.

Cabrera-Brufau M, Arin L, Sala MM, Cermeño P, Marrasé C. Diatom dominance enhances resistance of phytoplanktonic POM to mesopelagic microbial decomposition. Frontiers in Marine Science 2021; 8: 683354.

Cai Y, Guo L, Wang X, Aiken G. Abundance, stable isotopic composition, and export fluxes of DOC, POC, and DIC from the Lower Mississippi River during 2006–2008. Journal of Geophysical Research: Biogeosciences 2015; 120: 2273-2288.

Callahan BJ, McMurdie PJ, Rosen MJ, Han AW, Johnson AJA, Holmes SP. DADA2: high-resolution sample inference from Illumina amplicon data. Nature Methods 2016; 13: 581-583.

Chen B, Liu H, Landry MR, DaI M, Huang B, Sune J. Close coupling between phytoplankton growth and microzooplankton grazing in the western South China Sea. Limnology and Oceanography 2009; 54: 1084-1097.

Chen J, Li Y, Jing H, Zhang X, Xu Z, Xu J, et al. Genomic and transcriptomic evidence for the diverse adaptations of *Synechococcus* subclusters 5.2 and 5.3 to mesoscale eddies. New Phytologist 2022; 233: 1828-1842.

Cruz BN, Neuer S. Heterotrophic bacteria enhance the aggregation of the marine picocyanobacteria *Prochlorococcus* and *Synechococcus*. Frontiers in Microbiology 2019; 10: 1864.

Csardi G, Nepusz T, Traag V, Horvát S, Zanini F, Noom D, et al. igraph: network analysis and visualization in R, 2023. . https://CRAN.R-

project.org/package=igraph.

Dafner EV. Segmented continuous-flow analyses of nutrient in seawater: Intralaboratory comparison of Technicon AutoAnalyzer II and Bran+ Luebbe Continuous Flow AutoAnalyzer III. Limnology and Oceanography: Methods 2015; 13: 511-520.

Dalpadado P, Roxy MK, Arrigo KR, van Dijken GL, Chierici M, Ostrowski M, et al. Rapid climate change alters the environment and biological production of the Indian Ocean. Science of The Total Environment 2024; 906: 167342.

De Martini F, Neuer S, Hamill D, Robidart J, Lomas MW. Clade and strain specific contributions of *Synechococcus* and *Prochlorococcus* to carbon export in the Sargasso Sea. Limnology and Oceanography 2018; 63: S448-S457.

Deng W, Cruz BN, Neuer S. Effects of nutrient limitation on cell growth, TEP production and aggregate formation of marine *Synechococcus*. Aquatic Microbial Ecology 2016; 78: 39-49.

Deng W, Monks L, Neuer S. Effects of clay minerals on the aggregation and subsequent settling of marine *Synechococcus*. Limnology and Oceanography 2015; 60: 805-816.

Dufresne A, Ostrowski M, Scanlan DJ, Garczarek L, Mazard S, Palenik BP, et al. Unraveling the genomic mosaic of a ubiquitous genus of marine Cyanobacteria. Genome Biology 2008; 9: R90.

DuRand MD, Olson RJ, Chisholm SW. Phytoplankton population dynamics at the Bermuda Atlantic Time-series station in the Sargasso Sea. Deep Sea Research

Part II: Topical Studies in Oceanography 2001; 48: 1983-2003.

Durante G, Basset A, Stanca E, Roselli L. Allometric scaling and morphological variation in sinking rate of phytoplankton. Journal of Phycology 2019; 55: 1386-1393.

Flombaum P, Gallegos JL, Gordillo RA, Rincón J, Zabala LL, Jiao N, et al. Present and future global distributions of the marine Cyanobacteria *Prochlorococcus* and *Synechococcus*. Proceedings of the National Academy of Sciences 2013; 110: 9824-9829.

Flombaum P, Martiny AC. Diverse but uncertain responses of picophytoplankton lineages to future climate change. Limnology and Oceanography 2021; 66: 4171-4181.

Fox J, Weisberg S. An R companion to applied regression. Vol 1. Thousand Oaks, California, USA: Sage, 2019. https://socialsciences.mcmaster.ca/jfox/Books/Companion/

Hamm CE. Interactive aggregation and sedimentation of diatoms and clay-sized lithogenic material. Limnology and Oceanography 2002; 47: 1790-1795.

Huang Y, Liu X, Laws EA, Chen B, Li Y, Xie Y, et al. Effects of increasing atmospheric CO_2 on the marine phytoplankton and bacterial metabolism during a bloom: A coastal mesocosm study. Science of The Total Environment 2018; 633: 618-629.

Iversen MH, Ploug H. Ballast minerals and the sinking carbon flux in the ocean: carbon-specific respiration rates and sinking velocity of marine snow

aggregates. Biogeosciences 2010; 7: 2613-2624.

Kembel SW, Cowan PD, Helmus MR, Cornwell WK, Morlon H, Ackerly DD, et al. Picante: R tools for integrating phylogenies and ecology. Bioinformatics 2010; 26: 1463-1464.

Kolde R. pheatmap: pretty heatmaps, 2019. https://CRAN.R-project.org/package=pheatmap.

Kumar A, Ng DHP, Wu Y, Cao B. Microbial Community Composition and Putative Biogeochemical Functions in the Sediment and Water of Tropical Granite Quarry Lakes. Microbial Ecology 2019; 77: 1-11.

Li F, Burger A, Eppley JM, Poff KE, Karl DM, DeLong EF. Planktonic microbial signatures of sinking particle export in the open ocean's interior. Nature Communications 2023a; 14: 7177.

Li H, Feng X, Xiong T, Shao W, Wu W, Zhang Y. Particulate organic carbon released during macroalgal growth Has significant carbon sequestration potential in the ocean. Environmental Science & Technology 2023b.

Liaw A, Wiener M. Classification and regression by randomForest, 2002. https://CRAN.R-project.org/doc/Rnews/.

Liu H, Jing H, Wong THC, Chen B. Co-occurrence of phycocyanin-and phycoerythrin-rich *Synechococcus* in subtropical estuarine and coastal waters of Hong Kong. Environmental Microbiology Reports 2014; 6: 90-99.

Liu SM, Li LW, Zhang GL, Liu Z, Yu Z, Ren JL. Impacts of human activities on nutrient transports in the Huanghe (Yellow River) estuary. Journal of

Hydrology 2012; 430: 103-110.

Louca S, Parfrey LW, Doebeli M. Decoupling function and taxonomy in the global ocean microbiome. Science 2016; 353: 1272-1277.

Mackey KRM, Post AF, McIlvin MR, Saito MA. Physiological and proteomic characterization of light adaptations in marine *Synechococcus*. Environmental Microbiology 2017; 19: 2348-2365.

Mao F, Li W, Sim ZY, He Y, Chen Q, Yew-Hoong Gin K. Phycocyanin-rich *Synechococcus* dominates the blooms in a tropical estuary lake. Journal of Environmental Management 2022; 311: 114889.

Marie D, Partensky F, Jacquet S, Vaulot D. Enumeration and cell cycle analysis of natural populations of marine picoplankton by flow cytometry using the nucleic acid stain SYBR Green I. Applied and Environmental Microbiology 1997; 63: 186-193.

Mei W, Yu G, Greenwell BM. ggtrendline: Add Trendline and Confidence Interval to 'ggplot', 2022. https://CRAN.R-project.org/package=ggtrendline.

Morán XAG, LÓPEZ-URRUTIA Á, CALVO-DÍAZ A, Li WK. Increasing importance of small phytoplankton in a warmer ocean. Global Change Biology 2010; 16: 1137-1144.

Müller CL, Bonneau R, Kurtz Z. Generalized stability approach for regularized graphical models. arXiv preprint arXiv:1605.07072 2016.

Nair S, Zhang Z, Li H, Zhao H, Shen H, Kao S-J, et al. Inherent tendency of *Synechococcus* and heterotrophic bacteria for mutualism on long-term

coexistence despite environmental interference. Science Advances 2022; 8: eabf4792.

Oksanen J, Simpson G, Blanchet F, Kindt R, Legendre P, Minchin P, et al. vegan: community ecology package. R package version 2.6-4, 2022. https://CRAN.R-project.org/package=vegan.

Ortega-Retuerta E, Mazuecos IP, Reche I, Gasol JM, Álvarez-Salgado XA, Álvarez M, et al. Transparent exopolymer particle (TEP) distribution and in situ prokaryotic generation across the deep Mediterranean Sea and nearby North East Atlantic Ocean. Progress in Oceanography 2019; 173: 180-191.

Parks DH, Tyson GW, Hugenholtz P, Beiko RG. STAMP: statistical analysis of taxonomic and functional profiles. Bioinformatics 2014; 30: 3123-3124.

Pedersen TL. patchwork: the composer of plots, 2023. https://CRAN.R-project.org/package=patchwork.

Revelle W. psych: procedures for psychological, psychometric, and personality research, 2023. https://CRAN.R-project.org/package=psych.

Robeson MS II, O'Rourke DR, Kaehler BD, Ziemski M, Dillon MR, Foster JT, et al. RESCRIPt: Reproducible sequence taxonomy reference database management. PLoS Computational Biology 2021; 17: e1009581.

Ruber J, Geist J, Hartmann M, Millard A, Raeder U, Zubkov M, et al. Spatio-temporal distribution pattern of the picocyanobacterium *Synechococcus* in lakes of different trophic states: a comparison of flow cytometry and sequencing approaches. Hydrobiologia 2018; 811: 77-92.

Scanlan DJ, Ostrowski M, Mazard S, Dufresne A, Garczarek L, Hess WR, et al. Ecological genomics of marine picocyanobacteria. Microbiology and Molecular Biology Reviews 2009; 73: 249-299.

Simon M, Grossart H-P, Schweitzer B, Ploug H. Microbial ecology of organic aggregates in aquatic ecosystems. Aquatic Microbial Ecology 2002; 28: 175-211.

Six C, Ratin M, Marie D, Corre E. Marine *Synechococcus* picocyanobacteria: light utilization across latitudes. Proceedings of the National Academy of Sciences 2021; 118: e2111300118.

Stegen JC, Lin X, Fredrickson JK, Chen X, Kennedy DW, Murray CJ, et al. Quantifying community assembly processes and identifying features that impose them. The ISME Journal 2013; 7: 2069-2079.

Sundberg C, Al-Soud WA, Larsson M, Alm E, Yekta SS, Svensson BH, et al. 454 pyrosequencing analyses of bacterial and archaeal richness in 21 full-scale biogas digesters. FEMS Microbiology Ecology 2013; 85: 612-626.

Syvitski JP, Kettner A. Sediment flux and the Anthropocene. Philosophical Transactions of the Royal Society A: Mathematical, Physical and Engineering Sciences 2011; 369: 957-975.

Te SH, Kok JWK, Luo R, You L, Sukarji NH, Goh KC, et al. Coexistence of *Synechococcus* and microcystis blooms in a tropical urban reservoir and their links with microbiomes. Environmental Science & Technology 2023; 57: 1613-1624.

Tian S, Li Z, Wang Z, Jiang E, Wang W, Sun M. Mineral composition and particle size distribution of river sediment and loess in the middle and lower Yellow River. International Journal of Sediment Research 2021; 36: 392-400.

Timmermann A, Jin F-F. Phytoplankton influences on tropical climate. Geophysical Research Letters 2002; 29: 19-1-19-4.

Tréguer P, Bowler C, Moriceau B, Dutkiewicz S, Gehlen M, Aumont O, et al. Influence of diatom diversity on the ocean biological carbon pump. Nature Geoscience 2018; 11: 27-37.

Tsai A-Y, Gong G-C, Sanders RW, Chiang K-P, Chao C-F. Heterotrophic bacterial and *Synechococcus* spp. Growth and mortality along the inshore-offshore in the East China Sea in summer. Journal of Oceanography 2012; 68: 151-162.

Wang J, Shi B, Zhao E, Yuan Q, Chen X. The long-term spatial and temporal variations of sediment loads and their causes of the Yellow River Basin. Catena 2022a; 209: 105850.

Wang H, Wu X, Bi N, Li S, Yuan P, Wang A, et al. Impacts of the dam-orientated water-sediment regulation scheme on the lower reaches and delta of the Yellow River (Huanghe): A review. Global and Planetary Change 2017; 157: 93-113.

Wang S, Fu B, Piao S, Lü Y, Ciais P, Feng X, et al. Reduced sediment transport in the Yellow River due to anthropogenic changes. Nature Geoscience 2016; 9: 38-41.

Wang T, Chen X, Li J, Qin S. Phylogenetic structure of *Synechococcus* assemblages

and its environmental determinants in the bay and strait areas of a continental sea. Frontiers in Microbiology 2022b; 13: 757896.

Wang T, Li J, Jing H, Qin S. Picocyanobacterial *Synechococcus* in marine ecosystem: Insights from genetic diversity, global distribution, and potential function. Marine Environmental Research 2022c: 105622.

Wang T, Xia X, Chen J, Liu H, Jing H. Spatio-temporal variation of *Synechococcus* assemblages at DNA and cDNA levels in the tropical estuarine and coastal waters. Frontiers in Microbiology 2022d; 13: 837037.

Wei W, Chen X, Weinbauer MG, Jiao N, Zhang R. Reduced bacterial mortality and enhanced viral productivity during sinking in the ocean. The ISME Journal 2022; 16: 1668-1675.

Wen T, Xie P, Yang S, Niu G, Liu X, Ding Z, et al. ggClusterNet: An R package for microbiome network analysis and modularity-based multiple network layouts. iMeta 2022; 1: e32.

Wickham H, François R, Henry L, Müller K, Vaughan D. dplyr: A Grammar of Data Manipulation, 2023. https://CRAN.R-project.org/package=dplyr.

Worden AZ, Binder BJ. Application of dilution experiments for measuring growth and mortality rates among *Prochlorococcus* and *Synechococcus* populations in oligotrophic environments. Aquatic Microbial Ecology 2003; 30: 159-174.

Xia X, Partensky F, Garczarek L, Suzuki K, Guo C, Yan Cheung S, et al. Phylogeography and pigment type diversity of *Synechococcus* Cyanobacteria in surface waters of the northwestern Pacific Ocean. Environmental

Microbiology 2017; 19: 142-158.

Xia X, Zheng Q, Leung SK, Wang Y, Lee PY, Jing H, et al. Distinct metabolic strategies of the dominant heterotrophic bacterial groups associated with marine *Synechococcus*. Science of The Total Environment 2021; 798: 149208.

Xie R, Wang Y, Chen Q, Guo W, Jiao N, Zheng Q. Coupling between carbon and nitrogen metabolic processes mediated by coastal microbes in *Synechococcus*-derived organic matter addition incubations. Frontiers in Microbiology 2020; 11: 1041.

Yuan MM, Guo X, Wu L, Zhang Y, Xiao N, Ning D, et al. Climate warming enhances microbial network complexity and stability. Nature Climate Change 2021; 11: 343-348.

Yuan P, Liu D. Proposing a potential strategy concerning Mineral-enhanced Biological Pump (MeBP) for improving Ocean Iron Fertilization (OIF). Applied Clay Science 2021; 207: 106096.

Zamanillo M, Ortega-Retuerta E, Nunes S, Rodríguez-Ros P, Dall'Osto M, Estrada M, et al. Main drivers of transparent exopolymer particle distribution across the surface Atlantic Ocean. Biogeosciences 2019; 16: 733-749.

Zhang Y-Y, Ling J, Yang Q-S, Wang Y-S, Sun C-C, Sun H-Y, et al. The diversity of coral associated bacteria and the environmental factors affect their community variation. Ecotoxicology 2015; 24: 1467-1477.

Zhang Z, Tang L, Liang Y, Li G, Li H, Rivkin RB, et al. The relationship between two *Synechococcus* strains and heterotrophic bacterial communities and its

associated carbon flow. Journal of Applied Phycology 2021; 33: 953-966.

Zhao Z, Gonsior M, Luek J, Timko S, Ianiri H, Hertkorn N, et al. Picocyanobacteria and deep-ocean fluorescent dissolved organic matter share similar optical properties. Nature Communications 2017; 8: 1-10.

Zheng Q, Wang Y, Xie R, Lang AS, Liu Y, Lu J, et al. Dynamics of heterotrophic bacterial assemblages within *Synechococcus* cultures. Applied and Environmental Microbiology 2018; 84: e01517-17.

Figures

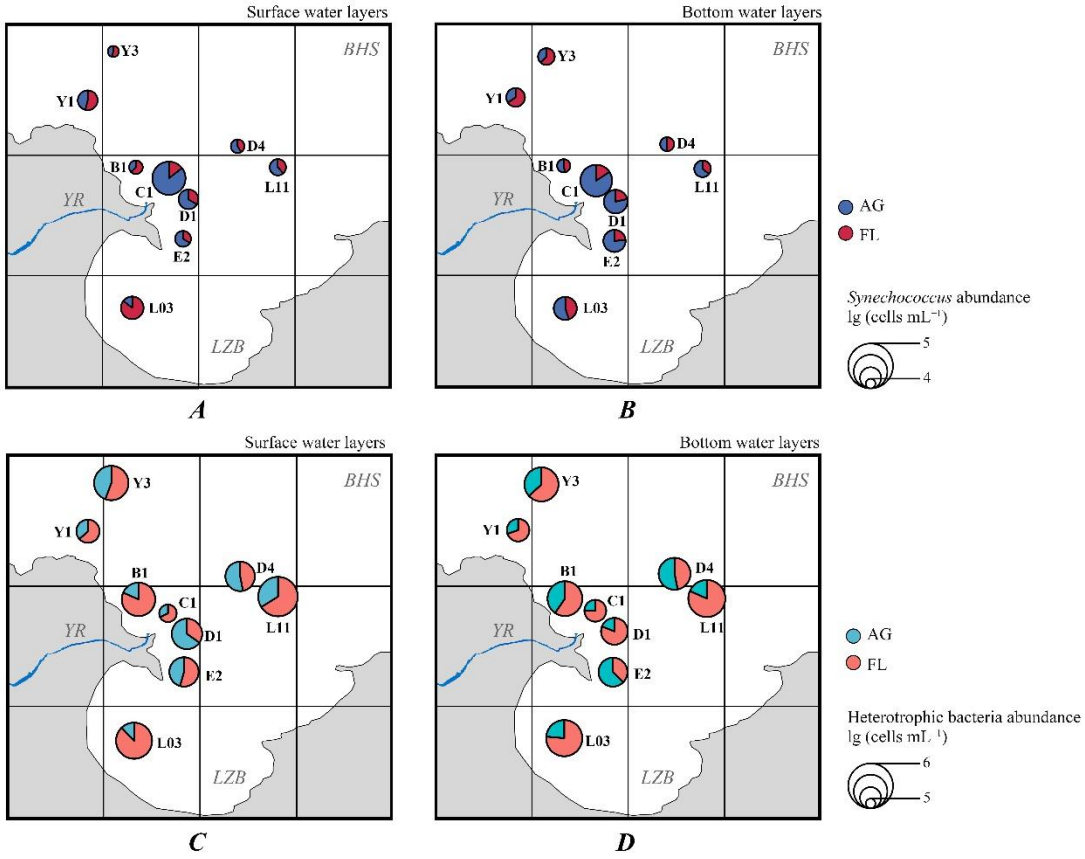

Figure 1 Spatial distribution of *Synechococcus* abundance in the surface (***A***) and bottom (***B***) water layers in the coastal waters of the Yellow River estuary. Spatial distribution of heterotrophic bacteria abundance in the surface (***C***) and bottom (***D***) water layers in the coastal waters of the Yellow River estuary. AG – aggregating; FL – free-living; BHS – Bohai Sea; LZB – Laizhou Bay; YR – Yellow River.

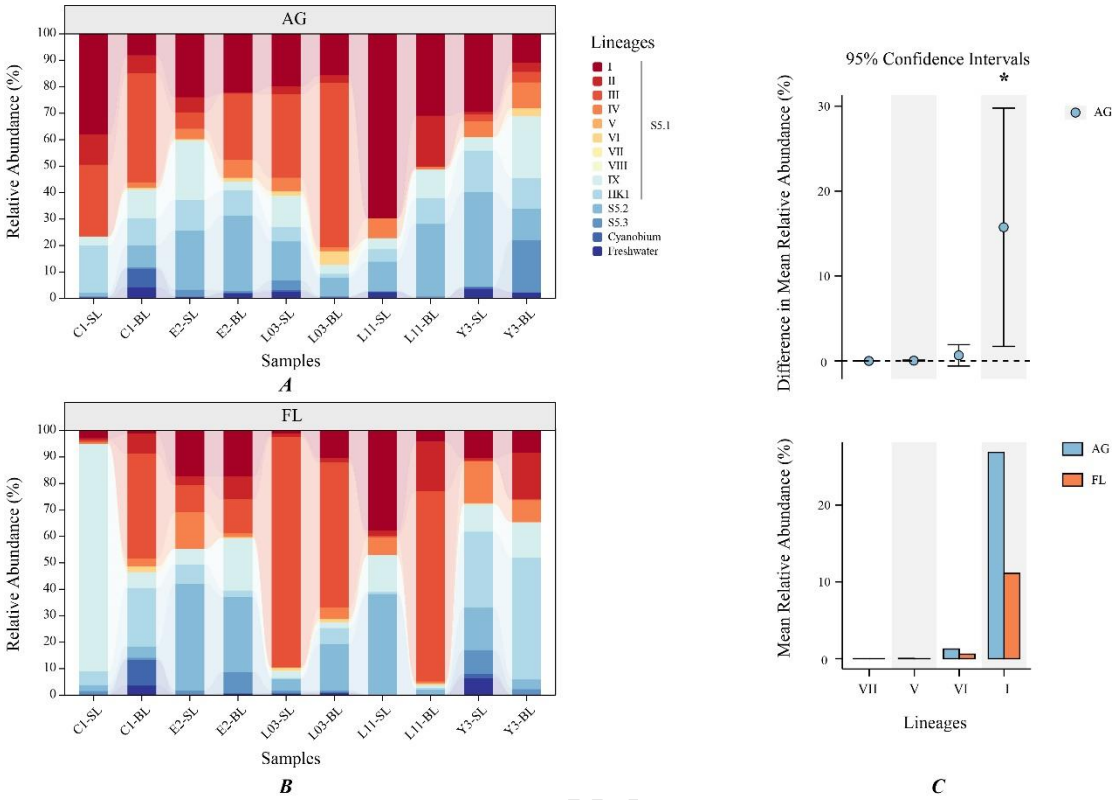

Figure 2 Relative abundances of aggregating (***A***) and free-living (***B***) *Synechococcus* lineages in the coastal waters of the Yellow River estuary. Significantly different taxonomic profiles between the AG and FL groups based on the Wilcoxon rank sum test (***C***). AG – aggregating; FL – free-living; SL – surface water layer; BL – bottom water layer; * – $p < 0.05$.

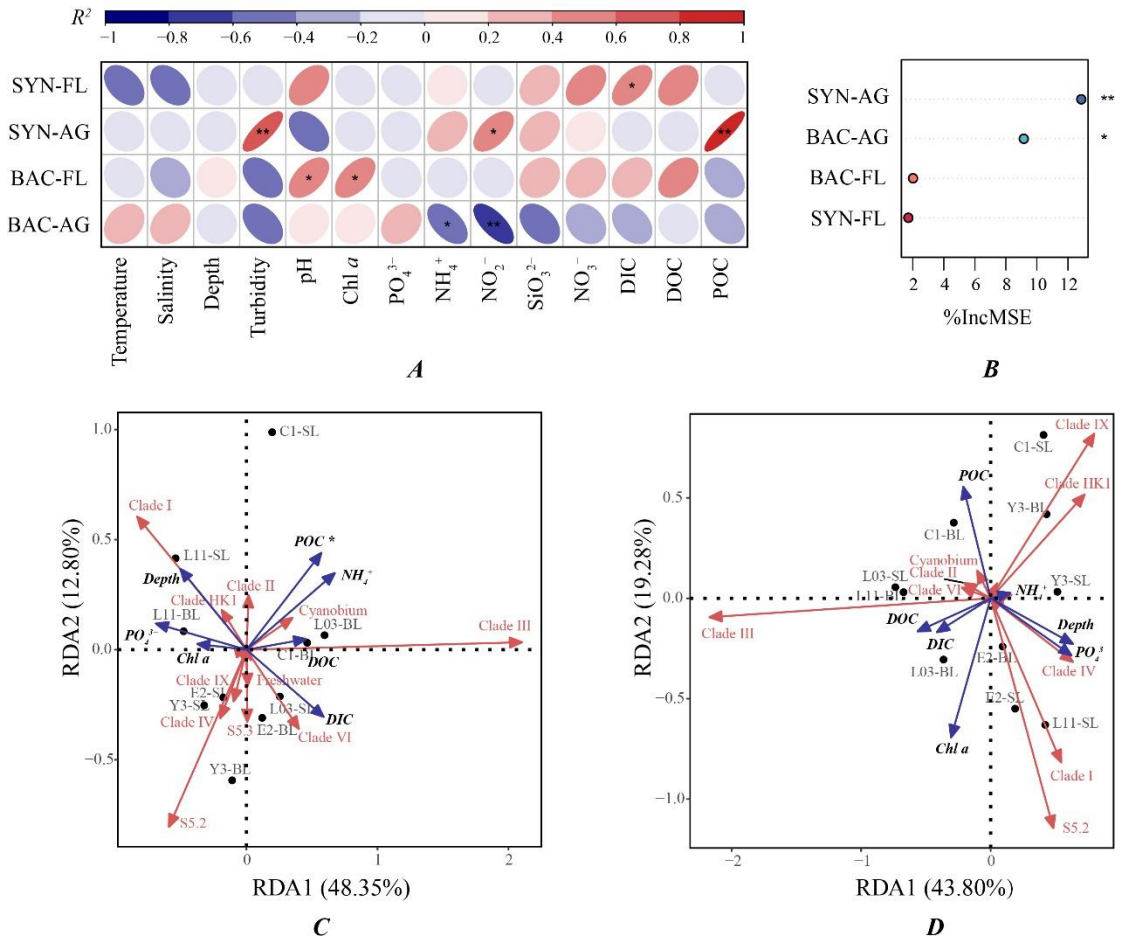

Figure 3 Spearman's correlations among microbial abundance and environmental variables (***A***). Percentage-increased MSE indicates the variable importance to POC in random forest regression (***B***). Correlation triplot based on an RDA depicting the relationship between the environmental variables and aggregating (***C***) or free-living (***D***) *Synechococcus* lineages at the clade level. SYN – *Synechococcus*; BAC – heterotrophic bacteria; AG – aggregating; FL – free-living; * – $p < 0.05$; ** – $p < 0.01$.

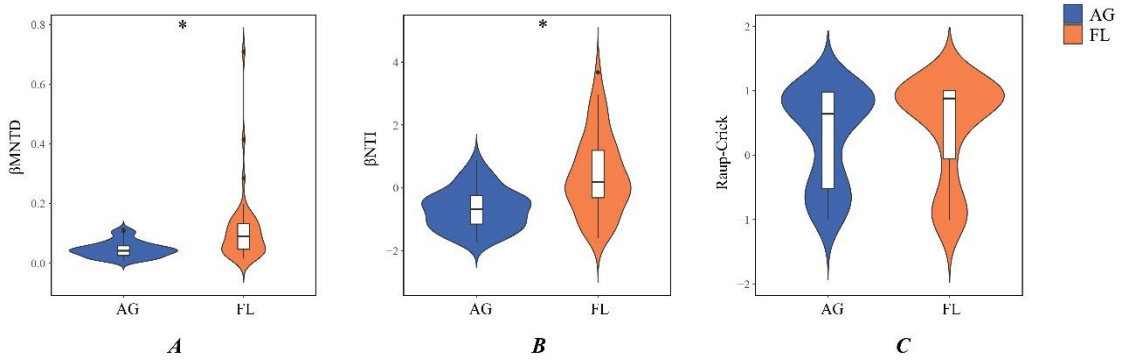

Figure 4 Beta-mean-nearest taxon distance (βMNTI) (***A***), beta nearest taxon index (βNTI) (***B***) and Raup–Crick index of aggregating and free-living *Synechococcus* communities in the coastal waters of the Yellow River estuary. AG – aggregating; FL – free-living; * – $p < 0.05$.

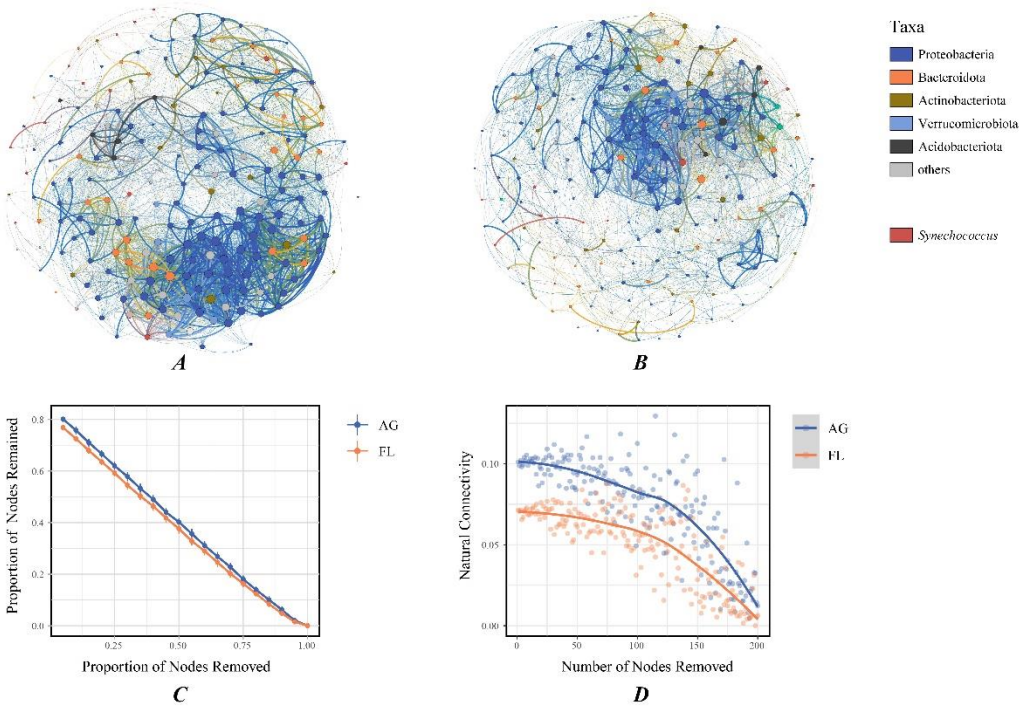

Figure 5 Co-occurrent network of aggregating (***A***) or free-living (***B***) microbial communities encompassing *Synechococcus* lineages and heterotrophic genera in the coastal waters of the Yellow River estuary. Dynamics of microbial network robustness, computed by calculating the proportion of nodes remained (***C***) and natural connectivity (***D***) after randomly removing a certain proportion or number of nodes.

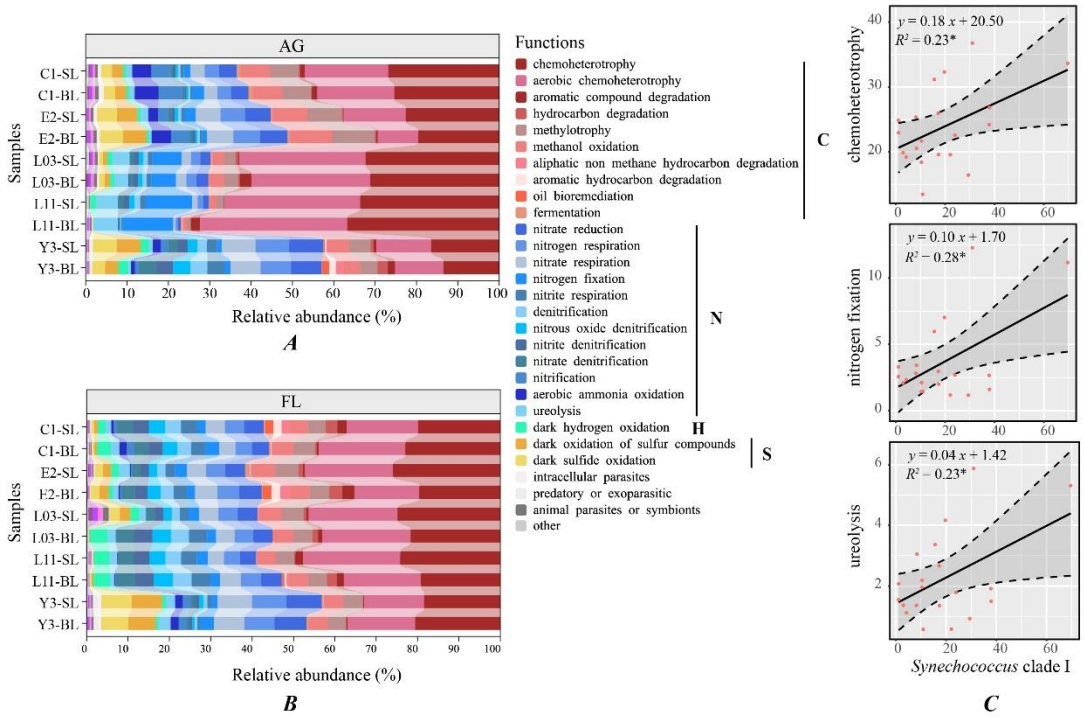

Figure 6 The relative abundance of the main ecological function profiles of AG (***A***) and FL (***B***) bacterial communities predicted using the FAPROTAX database in the coastal waters of the Yellow River estuary. The linear fitting relationships between Synechococcus clade I and ecological function profiles (***C***). AG – aggregating; FL – free-living; SL – surface water layer; BL – bottom water layer; C – carbon cycle; N – nitrogen cycle; H – hydrogen cycle; S – sulfur cycle; * – $p < 0.05$.

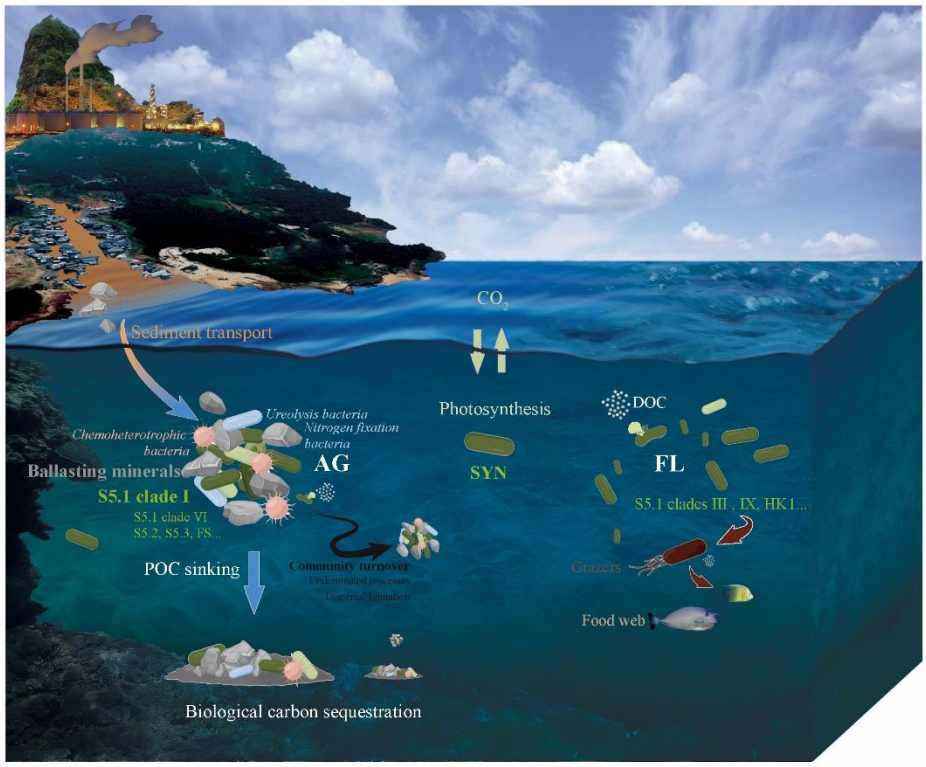

Figure 7 Schematic diagram illustrating carbon biogeochemical processes associated with the coupling of different lifestyles of *Synechococcus* and co-occurring functional heterotrophic bacteria in the coastal waters of the estuary with adequate ballasting minerals. SYN – *Synechococcus*; AG – aggregating; FL – free-living; DOC – dissolved organic carbon; POC – particulate organic carbon.

Author contributions

Conceptualization: TW, JLL, and SQ; Funding acquisition: JLL; Investigation: TW; Methodology: TW and TZ; Resources: YDX; Supervision: JLL and SQ; Visualization: TW; Writing – original draft: TW; Writing – review & editing: JLL and SQ.

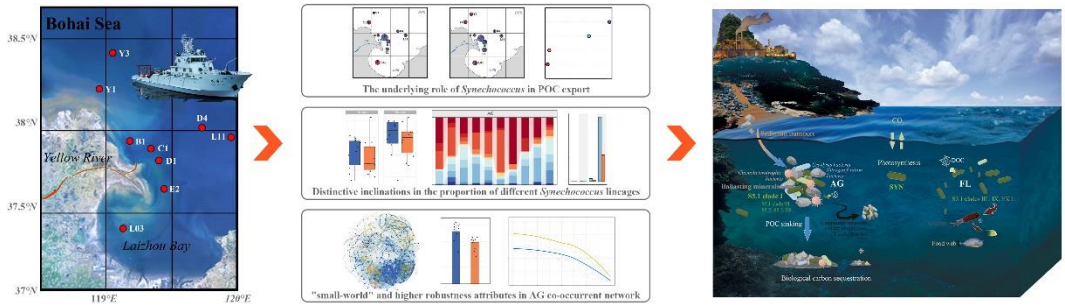

Graphical abstract

Highlights

- Terrigenous sediment transport has an important effect on particle organic carbon export of *Synechococcus* in coastal estuarine waters
- Distinct *Synechococcus* lineages exhibited different preferences between aggregating and free-living lifestyles
- Carbon and nitrogen metabolism coupling between *Synechococcus* and bacteria could promote the assembling of aggregations